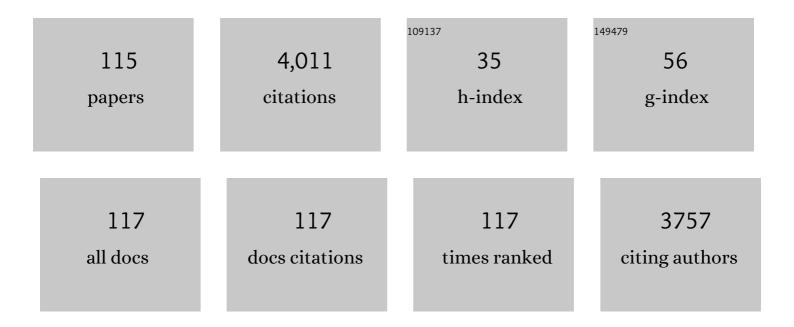
List of Publications by Year in descending order

Source: https://exaly.com/author-pdf/4516993/publications.pdf Version: 2024-02-01



ΙΝΟΗΛΝ ΡΛΝ

#	Article	lF	CITATIONS
1	The thickness of native oxides on aluminum alloys and single crystals. Applied Surface Science, 2015, 349, 826-832.	3.1	174
2	Depletion effects at phase boundaries in 2205 duplex stainless steel characterized with SKPFM and TEM/EDS. Corrosion Science, 2009, 51, 1850-1860.	3.0	170
3	Direct Electrochemical Synthesis of Reduced Graphene Oxide (rGO)/Copper Composite Films and Their Electrical/Electroactive Properties. ACS Applied Materials & Interfaces, 2014, 6, 7444-7455.	4.0	127
4	Study of nobility of chromium nitrides in isothermally aged duplex stainless steels by using SKPFM and SEM/EDS. Corrosion Science, 2010, 52, 179-186.	3.0	120
5	Influence of metal carbides on dissolution behavior of biomedical CoCrMo alloy: SEM, TEM and AFM studies. Electrochimica Acta, 2011, 56, 9413-9419.	2.6	112
6	Layered double hydroxide (LDH) for multi-functionalized corrosion protection of metals: A review. Journal of Materials Science and Technology, 2022, 102, 232-263.	5.6	112
7	Silane–parylene coating for improving corrosion resistance of stainless steel 316L implant material. Corrosion Science, 2011, 53, 296-301.	3.0	111
8	Localized corrosion behaviour of reinforcement steel in simulated concrete pore solution. Corrosion Science, 2009, 51, 2130-2138.	3.0	102
9	Electrochemical and AFM studies of mussel adhesive protein (Mefp-1) as corrosion inhibitor for carbon steel. Electrochimica Acta, 2011, 56, 1636-1645.	2.6	87
10	Determination of instantaneous corrosion rates and runoff rates of copper from naturally patinated copper during continuous rain events. Corrosion Science, 2002, 44, 2131-2151.	3.0	86
11	Influence of polyaniline and ceria nanoparticle additives on corrosion protection of a UV-cure coating on carbon steel. Corrosion Science, 2014, 84, 189-197.	3.0	84
12	A FEM model for investigation of micro-galvanic corrosion of Al alloys and effects of deposition of corrosion products. Electrochimica Acta, 2016, 192, 310-318.	2.6	76
13	Electrochemical behavior and anticorrosion properties of modified polyaniline dispersed in polyvinylacetate coating on carbon steel. Electrochimica Acta, 2008, 53, 4239-4247.	2.6	75
14	Scanning Kelvin probe force microscopy study of chromium nitrides in 2507 super duplex stainless steel—Implications and limitations. Electrochimica Acta, 2011, 56, 1792-1798.	2.6	75
15	On the Volta potential measured by SKPFM – fundamental and practical aspects with relevance to corrosion science. Corrosion Engineering Science and Technology, 2019, 54, 185-198.	0.7	73
16	Corrosion protection by hydrophobic silica particle-polydimethylsiloxane composite coatings. Corrosion Science, 2015, 99, 89-97.	3.0	69
17	The effect of superhydrophobic wetting state on corrosion protection – The AKD example. Journal of Colloid and Interface Science, 2013, 412, 56-64.	5.0	68
18	First-Principle Calculation of Volta Potential of Intermetallic Particles in Aluminum Alloys and Practical Implications. Journal of the Electrochemical Society, 2017, 164, C465-C473.	1.3	61

#	Article	IF	CITATIONS
19	Real-Time and Online Lubricating Oil Condition Monitoring Enabled by Triboelectric Nanogenerator. ACS Nano, 2021, 15, 11869-11879.	7.3	56
20	In-situ AFM and EIS study of a solventborne alkyd coating with nanoclay for corrosion protection of carbon steel. Progress in Organic Coatings, 2015, 87, 179-188.	1.9	54
21	Correlative Microstructure Analysis and In Situ Corrosion Study of AISI 420 Martensitic Stainless Steel for Plastic Molding Applications. Journal of the Electrochemical Society, 2017, 164, C85-C93.	1.3	52
22	Characterization of Phases in Duplex Stainless Steel by Magnetic Force Microscopy/Scanning Kelvin Probe Force Microscopy. Electrochemical and Solid-State Letters, 2008, 11, C41.	2.2	51
23	Study of corrosion behavior of a 22% Cr duplex stainless steel: Influence of nano-sized chromium nitrides and exposure temperature. Electrochimica Acta, 2013, 113, 280-289.	2.6	50
24	Corrosion Inhibition of Aluminum Alloy AA6063-T5 by Vanadates: Microstructure Characterization and Corrosion Analysis. Journal of the Electrochemical Society, 2018, 165, C116-C126.	1.3	49
25	In Situ and Operando AFM and EIS Studies of Anodization of Al 6060: Influence of Intermetallic Particles. Journal of the Electrochemical Society, 2016, 163, C609-C618.	1.3	48
26	Numerical Simulation of Micro-Galvanic Corrosion in Al Alloys: Effect of Geometric Factors. Journal of the Electrochemical Society, 2017, 164, C75-C84.	1.3	48
27	Toward Homogeneous Nanostructured Polyaniline/Resin Blends. ACS Applied Materials & Interfaces, 2011, 3, 1681-1691.	4.0	45
28	Hydrogen embrittlement of super duplex stainless steel – Towards understanding the effects of microstructure and strain. International Journal of Hydrogen Energy, 2018, 43, 12543-12555.	3.8	44
29	Active corrosion protection by conductive composites of polyaniline in a UV-cured polyester acrylate coating. Progress in Organic Coatings, 2016, 90, 154-162.	1.9	43
30	Corrosion inhibition of aluminium alloy AA6063-T5 by vanadates: Local surface chemical events elucidated by confocal Raman micro-spectroscopy. Corrosion Science, 2019, 148, 237-250.	3.0	43
31	Tafel slopes used in monitoring of copper corrosion in a bentonite/groundwater environment. Corrosion Science, 2005, 47, 3267-3279.	3.0	42
32	Study of PANI-MeSA conducting polymer dispersed in UV-curing polyester acrylate on galvanized steel as corrosion protection coating. Progress in Organic Coatings, 2011, 70, 108-115.	1.9	41
33	Corrosion protective properties of cellulose nanocrystals reinforced waterborne acrylate-based composite coating. Corrosion Science, 2019, 155, 186-194.	3.0	40
34	Influence of Grain Boundaries on Dissolution Behavior of a Biomedical CoCrMo Alloy: In-Situ Electrochemical-Optical, AFM and SEM/TEM Studies. Journal of the Electrochemical Society, 2012, 159, C422-C427.	1.3	39
35	Local surface mechanical properties of PDMS-silica nanocomposite probed with Intermodulation AFM. Composites Science and Technology, 2017, 150, 111-119.	3.8	37
36	Redefining passivity breakdown of super duplex stainless steel by electrochemical operando synchrotron near surface X-ray analyses. Npj Materials Degradation, 2019, 3, .	2.6	36

#	Article	IF	CITATIONS
37	Nanoscale Electrical and Mechanical Characteristics of Conductive Polyaniline Network in Polymer Composite Films. ACS Applied Materials & Interfaces, 2014, 6, 19168-19175.	4.0	35
38	Electrochemical impedance spectroscopy of pure copper exposed in bentonite under oxic conditions. Electrochimica Acta, 2011, 56, 7862-7870.	2.6	34
39	Thickness and composition of native oxides and near-surface regions of Ni superalloys. Journal of Alloys and Compounds, 2022, 895, 162657.	2.8	33
40	Multifunctional commercially pure titanium for the improvement of bone integration: Multiscale topography, wettability, corrosion resistance and biological functionalization. Materials Science and Engineering C, 2016, 60, 384-393.	3.8	32
41	In-situ synchrotron GIXRD study of passive film evolution on duplex stainless steel in corrosive environment. Corrosion Science, 2018, 141, 18-21.	3.0	32
42	An electrochemical impedance spectroscopy study of copper in a bentonite/saline groundwater environment. Electrochimica Acta, 2008, 53, 7556-7564.	2.6	31
43	In situ confocal Raman micro-spectroscopy and electrochemical studies of mussel adhesive protein and ceria composite film on carbon steel in salt solutions. Electrochimica Acta, 2013, 107, 276-291.	2.6	31
44	Anodisation of aluminium alloy AA7075 – Influence of intermetallic particles on anodic oxide growth. Corrosion Science, 2020, 164, 108319.	3.0	31
45	Nano-scale mechanical and wear properties of a waterborne hydroxyacrylic-melamine anti-corrosion coating. Applied Surface Science, 2018, 457, 548-558.	3.1	29
46	Engineering of bone fixation metal implants biointerface—Application of parylene C as versatile protective coating. Materials Science and Engineering C, 2012, 32, 2431-2435.	3.8	28
47	In situ investigations of Fe3+ induced complexation of adsorbed Mefp-1 protein film on iron substrate. Journal of Colloid and Interface Science, 2013, 404, 62-71.	5.0	28
48	In-Situ AFM and EIS Study of Waterborne Acrylic Latex Coatings for Corrosion Protection of Carbon Steel. Journal of the Electrochemical Society, 2015, 162, C55-C63.	1.3	28
49	Atmospheric corrosion of Cu, Zn, and Cu–Zn alloys protected by self-assembled monolayers of alkanethiols. Surface Science, 2016, 648, 170-176.	0.8	28
50	Passive film characterisation of duplex stainless steel using scanning Kelvin probe force microscopy in combination with electrochemical measurements. Npj Materials Degradation, 2019, 3, .	2.6	28
51	Volta Potential EvolutionÂof Intermetallics in Aluminum Alloy MicrostructureÂUnder Thin Aqueous Adlayers: A combined DFT and Experimental Study. Topics in Catalysis, 2018, 61, 1169-1182.	1.3	26
52	In Situ AFM and Electrochemical Study of a Waterborne Acrylic Composite Coating with CeO ₂ Nanoparticles for Corrosion Protection of Carbon Steel. Journal of the Electrochemical Society, 2015, 162, C610-C618.	1.3	25
53	Micro-galvanic corrosion of Cu/Ru couple in potassium periodate (KIO 4) solution. Corrosion Science, 2018, 137, 184-193.	3.0	25
54	A DFT-Study of Cl Ingress into α-Al ₂ O ₃ (0001) and Al(111) and Its Possible Influence on Localized Corrosion of Al. Journal of the Electrochemical Society, 2019, 166, C3124-C3130.	1.3	25

#	Article	IF	CITATIONS
55	Nickel release from nickel particles in artificial sweat. Contact Dermatitis, 2007, 56, 325-330.	0.8	24
56	Numerical Simulation of Micro-Galvanic Corrosion of Al Alloys: Effect of Chemical Factors. Journal of the Electrochemical Society, 2017, 164, C768-C778.	1.3	24
57	Thin Composite Films of Mussel Adhesive Proteins and Ceria Nanoparticles on Carbon Steel for Corrosion Protection. Journal of the Electrochemical Society, 2012, 159, C364-C371.	1.3	23
58	Micro-Galvanic Corrosion Effects on Patterned Copper-Zinc Samples during Exposure in Humidified Air Containing Formic Acid. Journal of the Electrochemical Society, 2013, 160, C423-C431.	1.3	23
59	Localized Corrosion of Binary Mg–Ca Alloy in 0.9Âwt% Sodium Chloride Solution. Acta Metallurgica Sinica (English Letters), 2016, 29, 46-57.	1.5	23
60	Real-Time Corrosion Monitoring of Aluminum Alloy Using Scanning Kelvin Probe Force Microscopy. Journal of the Electrochemical Society, 2020, 167, 081502.	1.3	23
61	Microstructure influence on corrosion behavior of a Fe–Cr–V–N tool alloy studied by SEM/EDS, scanning Kelvin force microscopy and electrochemical measurement. Corrosion Science, 2013, 66, 153-159.	3.0	22
62	EIS and in situ AFM study of barrier property and stability of waterborne and solventborne clear coats. Progress in Organic Coatings, 2014, 77, 600-608.	1.9	22
63	In Situ AFM Study of Localized Corrosion Processes of Tempered AISI 420 Martensitic Stainless Steel: Effect of Secondary Hardening. Journal of the Electrochemical Society, 2017, 164, C810-C818.	1.3	22
64	Mussel-Inspired Graphene Film with Enhanced Durability as a Macroscale Solid Lubricant. ACS Applied Materials & Interfaces, 2019, 11, 31386-31392.	4.0	22
65	Characterization of Native Oxide and Passive Film on Austenite/Ferrite Phases of Duplex Stainless Steel Using Synchrotron HAXPEEM. Journal of the Electrochemical Society, 2019, 166, C3336-C3340.	1.3	22
66	Investigation and application of mussel adhesive protein nanocomposite film-forming inhibitor for reinforced concrete engineering. Corrosion Science, 2019, 153, 333-340.	3.0	22
67	Corrosion- and wear-resistant composite film of graphene and mussel adhesive proteins on carbon steel. Corrosion Science, 2020, 164, 108351.	3.0	22
68	Lateral variation of the native passive film on super duplex stainless steel resolved by synchrotron hard X-ray photoelectron emission microscopy. Corrosion Science, 2020, 174, 108841.	3.0	22
69	UVâ€curable acrylateâ€based nanocomposites: effect of polyaniline additives on the curing performance. Polymers for Advanced Technologies, 2013, 24, 668-678.	1.6	21
70	Long-term corrosion protection by a thin nano-composite coating. Applied Surface Science, 2015, 357, 2333-2342.	3.1	21
71	Numerical Simulation of Micro-Galvanic Corrosion in Al Alloys: Steric Hindrance Effect of Corrosion Product. Journal of the Electrochemical Society, 2017, 164, C1035-C1043.	1.3	21
72	Passivation characteristics of ultra-thin 316L foil in NaCl solutions. Journal of Materials Science and Technology, 2022, 127, 192-205.	5.6	21

#	Article	IF	CITATIONS
73	Corrosion Protection and Self-Healing of a Nanocomposite Film of Mussel Adhesive Protein and CeO ₂ Nanoparticles on Carbon Steel. Journal of the Electrochemical Society, 2016, 163, C545-C552.	1.3	20
74	Integration of electrochemical and synchrotron-based X-ray techniques for in-situ investigation of aluminum anodization. Electrochimica Acta, 2017, 241, 299-308.	2.6	19
75	Electrochemical, atomic force microscopy and infrared reflection absorption spectroscopy studies of pre-formed mussel adhesive protein films on carbon steel for corrosion protection. Thin Solid Films, 2012, 520, 7136-7143.	0.8	18
76	Controllable degradation of medical magnesium by electrodeposited composite films of mussel adhesive protein (Mefp-1) and chitosan. Journal of Colloid and Interface Science, 2016, 478, 246-255.	5.0	18
77	Towards the mechanism of electrochemical activity and self-healing of 1 wt% PTSA doped polyaniline in alkyd composite polymer coating: combined AFM-based studies. RSC Advances, 2016, 6, 19111-19127.	1.7	18
78	Probing the vertical profiles of potential in a thin layer of solution closed to electrode surface during localized corrosion of stainless steel. Corrosion Science, 2012, 61, 242-245.	3.0	17
79	Numerical simulation of micro-galvanic corrosion of Al alloys: Effect of density of Al(OH)3 precipitate. Electrochimica Acta, 2019, 324, 134847.	2.6	17
80	Influence of Surface Strain on Passive Film Formation of Duplex Stainless Steel and Its Degradation in Corrosive Environment. Journal of the Electrochemical Society, 2019, 166, C3071-C3080.	1.3	17
81	Octadecanethiol as Corrosion Inhibitor for Zinc and Patterned Zinc-Copper in Humidified Air with Formic Acid. Journal of the Electrochemical Society, 2014, 161, C330-C338.	1.3	16
82	Combining lithography and capillary techniques for local electrochemical property measurements. Electrochemistry Communications, 2018, 87, 53-57.	2.3	16
83	Insight into the Fabrication of ZnAl Layered Double Hydroxides Intercalated with Organic Anions and Their Corrosion Protection of Steel Reinforced Concrete. Journal of the Electrochemical Society, 2019, 166, C617-C623.	1.3	16
84	Direct Measurement of Colloidal Interactions between Polyaniline Surfaces in a UV-Curable Coating Formulation: The Effect of Surface Hydrophilicity/Hydrophobicity and Resin Composition. Langmuir, 2014, 30, 1045-1054.	1.6	15
85	Temperature-dependent surface nanomechanical properties of a thermoplastic nanocomposite. Journal of Colloid and Interface Science, 2017, 494, 204-214.	5.0	15
86	Corrosion inhibition of pre-formed mussel adhesive protein (Mefp-1) film to magnesium alloy. Corrosion Science, 2020, 164, 108309.	3.0	15
87	Corrosion-induced microstructure degradation of copper in sulfide-containing simulated anoxic groundwater studied by synchrotron high-energy X-ray diffraction and ab-initio density functional theory calculation. Corrosion Science, 2021, 184, 109390.	3.0	15
88	Tribological Properties Mapping: Local Variation in Friction Coefficient and Adhesion. Tribology Letters, 2013, 50, 387-395.	1.2	14
89	Metastable precursor structures in hydrogen-infused super duplex stainless steel microstructure – An operando diffraction experiment. Corrosion Science, 2020, 176, 109021.	3.0	14
90	Towards understanding micro-galvanic activities in localised corrosion of AA2099 aluminium alloy. Electrochimica Acta, 2021, 392, 139005.	2.6	13

#	Article	IF	CITATIONS
91	Studying the Passivity and Breakdown of Duplex Stainless Steels at Micrometer and Nanometer Scales – The Influence of Microstructure. Frontiers in Materials, 2020, 7, .	1.2	12
92	Corrosion Investigations of Ruthenium in Potassium Periodate Solutions Relevant for Chemical Mechanical Polishing. Journal of Electronic Materials, 2016, 45, 4067-4075.	1.0	11
93	Probing electrochemical mechanism of polyaniline and CeO2 nanoparticles in alkyd coating with in-situ electrochemical-AFM and IRAS. Progress in Organic Coatings, 2019, 132, 399-408.	1.9	11
94	Co-Adsorption of H2O, OH, and Cl on Aluminum and Intermetallic Surfaces and Its Effects on the Work Function Studied by DFT Calculations. Molecules, 2019, 24, 4284.	1.7	11
95	Comparative study of CNC and CNF as additives in waterborne acrylate-based anti-corrosion coatings. Journal of Dispersion Science and Technology, 2020, 41, 2037-2047.	1.3	11
96	In-Situ Time-Lapse SKPFM Investigation of Sensitized AA5083 Aluminum Alloy to Understand Localized Corrosion. Journal of the Electrochemical Society, 2020, 167, 141502.	1.3	11
97	Experimental and modelling study of the effect of tempering on the susceptibility to environment-assisted cracking of AISI 420 martensitic stainless steel. Corrosion Science, 2019, 148, 83-93.	3.0	10
98	Operando time- and space-resolved high-energy X-ray diffraction measurement to understand hydrogen-microstructure interactions in duplex stainless steel. Corrosion Science, 2020, 175, 108899.	3.0	10
99	Density Functional Theory Study of Influence of Oxide Thickness and Surface Alloying on Cl Migration within α-Al ₂ O ₃ . Journal of the Electrochemical Society, 2021, 168, 081508.	1.3	10
100	Microstructure and transformation temperatures in rapid solidified Ni–Ti alloys. Part II: The effect of copper addition. Journal of Alloys and Compounds, 2014, 589, 633-642.	2.8	9
101	Recent Development of Corrosion Protection Strategy Based on Mussel Adhesive Protein. Frontiers in Materials, 2019, 6, .	1.2	9
102	Time-resolved grazing-incidence X-ray diffraction measurement to understand the effect of hydrogen on surface strain development in super duplex stainless steel. Scripta Materialia, 2020, 187, 63-67.	2.6	8
103	Minuscule device for hydrogen generation/electrical energy collection system on aluminum alloy surface. International Journal of Hydrogen Energy, 2011, 36, 2855-2859.	3.8	7
104	Radial Spreading of Localized Corrosion-Induced Selective Leaching on α-Brass in Dilute NaCl Solution. Corrosion, 2013, 69, 468-476.	0.5	7
105	Role of microstructure on corrosion initiation of an experimental tool alloy: A Quantitative Nanomechanical Property Mapping study. Corrosion Science, 2014, 89, 236-241.	3.0	7
106	Corrosion Inhibition of Two Brass Alloys by Octadecanethiol in Humidified Air with Formic Acid. Corrosion, 2015, 71, 908-917.	0.5	6
107	Tunable Adsorption and Film Formation of Mussel Adhesive Protein by Potential Control. Langmuir, 2017, 33, 8749-8756.	1.6	6
108	Heating-Induced Enhancement of Corrosion Protection of Carbon Steel by a Nanocomposite Film Containing Mussel Adhesive Protein. Journal of the Electrochemical Society, 2017, 164, C188-C193.	1.3	6

#	Article	IF	CITATIONS
109	Hydrogen-Induced Micro-Strain Evolution in Super Duplex Stainless Steel—Correlative High-Energy X-Ray Diffraction, Electron Backscattered Diffraction, and Digital Image Correlation. Frontiers in Materials, 2022, 8, .	1.2	6
110	Temperature effect on mechanical strength and frictional properties of polytetrafluoroethyleneâ€based coreâ€shell nanocomposites. Journal of Applied Polymer Science, 2021, 138, 49929.	1.3	5
111	Investigation of Influence of Small Particles in MP35N on the Corrosion Resistance in Synthetic Biological Environment. Journal of the Electrochemical Society, 2009, 156, C341.	1.3	3
112	Experimental and Simulation Investigations of Copper Reduction Mechanism with and without Addition of SPS. Journal of the Electrochemical Society, 2018, 165, D604-D611.	1.3	3
113	Interactions in Composite Film Formation of Mefp-1/graphene on Carbon Steel. Coatings, 2021, 11, 1161.	1.2	2
114	Reply to Comment on "Corrosion-induced microstructure degradation of copper in sulfide-containing simulated anoxic groundwater studied by synchrotron high-energy X-ray diffraction and ab-initio density functional theory calculation― Corrosion Science, 2022, 199, 110183.	3.0	2
115	Relevance of implicit and explicit solvent in density-functional theory study of adsorption at electrochemical NaCl/Al interface. Materials Today Communications, 2022, 31, 103425.	0.9	1